Manuscript refereed by Dr Christian Kukla (Montanuniversitaet Leoben, Austria)

Design Guidelines For Green Parts Manufactured With Stainless Steel In The Filament Based Material Extrusion Process For Metals (MEX/M)

Karim Asami[1] karim.asami@tuhh.de; Dirk Herzog[1] dirk.herzog@tuhh.de; Bastian Bossen[1] bastian.bossen@tuhh.de; Leon Geyer[1] leon.geyer@tuhh.de; Clarissa Klemp[1] clarissa.klemp@tuhh.de, Claus Emmelmann[1] c.emmelmann@tuhh.de

[1]Hamburg University of Technology, Institute of Laser and System Technologies, Harburger Schloßstr. 28, 21079 Hamburg, Germany

Abstract

Filament-based material extrusion (MEX/M) presents a rapid and inexpensive alternative to e.g. metal injection molding, particularly for prototype production. The filament consists of metal powder in a plastic matrix and is melted and applied layer by layer until a so-called green body is created. These green parts are subsequently debinded and sintered at high temperatures to form a dense metal component. It is crucial to identify the material-specific and process-specific limits in order to be able to manufacture true to size. This paper therefore develops design guidelines for the MEX/M process for green part manufacturing for the widely used austenitic stainless steel AISI 316L (1.4404). Basic geometrical features such as walls, boreholes and overhangs are studied and influencing factors on the dimensional accuracy are assessed. Based on the results, recommendations for part design are presented.

Introduction

The filament-based material extrusion (MEX/M, also known Metal Fused-Filament Fabrication as per ISO 52900) has become popular over the last years in different fields such as functional prototyping and small scale fabrication [1]. One reason is the existing knowledge of the metal injection molding (MIM) and the fused deposition modelling (FDM) processes. Since the MEX/M process consists of the combination of both MIM and FDM processes it is easy to transfer and to add knowledge that has been previously accumulated. The main advantage compared to MIM is that no mold is needed and the time for its creation can be neglected. Therefore, the limitations in the design complexity of MEX/M-parts are not restricted due to the degree of freedom and the limited shape [2]. Another reason for the popularity is the larger availability of different filament-based materials and machines provided by different suppliers such as BASF SE [3], Virtual foundry [4], Anycubic [5], PT&A [6], Desktop Metal [7], Triditive [8] and Markforged [9]. The MEX/M process consists of three process steps: printing, debinding and sintering. While the debinding and sintering have been extensively studied through the injection molding process (see [10,11]) there hardly exist design studies in the printing step of MEX/M process [12]. Therefore, this paper investigates design features to develop a design catalogue for an accurate component design.

Materials and Methods

For this investigation different design features are introduced. The design limitations and recommendations identified in this paper are dependent on the material, the machine, the particular process parameters and environmental conditions. The basic geometrical elements used for the tests are typical features which occur in a number of industrial parts and have successfully been applied to established design guidelines for other AM processes [13,14,15]. The geometric properties are changed parameter wise to identify the manufacturing limits. Table 1 shows the investigated specimens.

Table 1: Developed specimens for the investigation.

Unsupported Walls 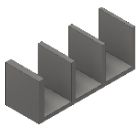	Horizontal Overhangs 
Width (mm): 10/24/32 Height (mm): 0.4/0.6/0.8/1/4.8/6.4/9.6/10/12/14.4/16/19.2 Thickness (mm): 0.1/0.2/…/0.5/0.7/0.8/1/1.2/1.6	Width, Thickness (mm): 5 Height (mm): 6 Overhang length a (mm): 0.3/0.5/1/2 Overhang height (mm): 3

Inclined Walls

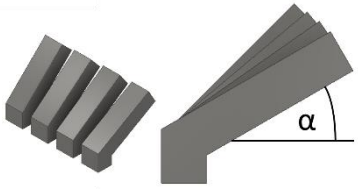

Width (mm): 10
Thickness (mm): 15
Height (mm): 20
Overhang angle α (°): 15,25,30,35,40,45,50

Bridges

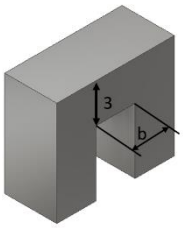

Width (mm): 5
Total Height (mm): 8
Total length (mm): 10+ b
Bridge distance b (mm): 0.3/0.5/1/2/3/5

Cylindrical rods

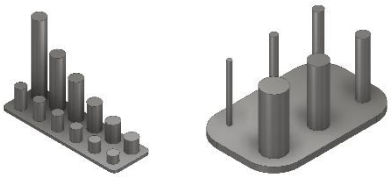

Diameter (mm): 0.8/1.2/1.6/2/3/4/5
Height (mm): 3,4,…,8/10/15/20/30

Vertical gaps

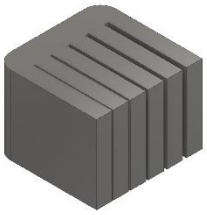

Width, Thickness (mm): 12
Height (mm): 10
Gap width (mm): 0.1, 0.2, …, 0.5

Horizontal boreholes

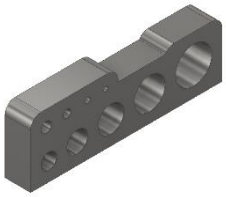

Width (mm): 5
Diameter (mm): 0.8, 1, 1.5, 2, 3, 4, 5, 6, 7

Vertical boreholes

Height (mm): 5
Diameter (mm): 0.8, 1, 1.5, 2, 2.5, 3

The specimens are manufactured with AISI 316L (1.4404) filament provided by the company PT&A (Dresden, Germany) with the starting powder composition illustrated in table 2 are provided by the manufacturer. The filament diameter is 2.85 mm with a tolerance of 0.05 mm.

Table 2: starting powder composition for 316-L (1.4404)
in weight %

Cr	**Ni**	**Mo**	**Mn**	**Si**	**P**	**S**	**C**	**F**
16.8	10.1	2.2	1.38	0.74	0.02	0.018	0.004	bal.

The components of the binder are not known. According to the manufacturer, debinding with acetone as solvent is recommended.

The test specimens are produced with the MEX/M process on a Renkforce RF 2000 (Conrad Electronic SE, Hirschau, Germany) 3D printer with 0.4 mm nozzle diameter using Simplify3D (Cincinnati, USA) slicer software. The extruder of this printer has been optimized for constant metal filament feeding. The process parameters are chosen to avoid typical printing errors known in FDM such as stringing [16], oozing [16], bridging [17], elephant foot [18], etc. These are the main influence factors for accurate printing, displayed in table 3. The distance and roughness measurements have been performed with a Keyence VK-X150 (Osaka, Japan) microscope, a caliper gauge and a feeler gauge. The specimens (green parts) have been measured at the edges and in the center of each feature. The roughness measurements for the inclined walls were performed on the downskin area, since this area is critical for a free overhang, where the material can sink. Line measurements have been made for the surface according to the method presented in [15].

Table 3: Printing parameters

Extrusion temperature (°C)	135
Heat bed temperature (°C)	40
Printing speed (mm/s)	2100
Extrusion multiplier	1.35
Skirt layer	2
Retraction distance (mm)	4.5
Layer height (mm)	0.2

Results and Discussion

The results from the experiments are given in figures 1-7 in the form of a comparison of the actual geometrical values with the respective target values. Each diagram shows the modeled parameter on the x-axis and the printed quantity as a percentage on the y-axis. For the overhang measurements the overhang angles are plotted over the mean roughness values Rz of the downskin area. Typical defects are additionally visualized using light microscope and photographic images.

Unsupported walls

Figure 1 (left) shows the percentual measurement results of modeled and fabricated heights for different lengths and widths. Furthermore, the differently developed widths at fixed length and height are shown (right). Walls with a width and length of 10 mm are created with a height between 0.4 mm and 4.8 mm. The walls with a width of 1.2 mm are created with a height between 7.2 mm and 14.4 mm. Walls with a width of 1.6 mm were in the range of 6.4 mm to 19.2 mm. All samples could be built and reached >95% of the designed target height with a height higher than 0.4 mm. For the samples with a width of 1.2 mm, the created height tends to decrease at 12 mm and 14.4 mm (gray bars). Figure 1 below shows different target thicknesses for fixed wall widths and lengths of 10 mm each. All specimens have been built up thicker than designed. From a thickness of 1 mm the over-extrusion is less than 20%. The thickness of 0.7 mm has been manufactured nearly as designed.

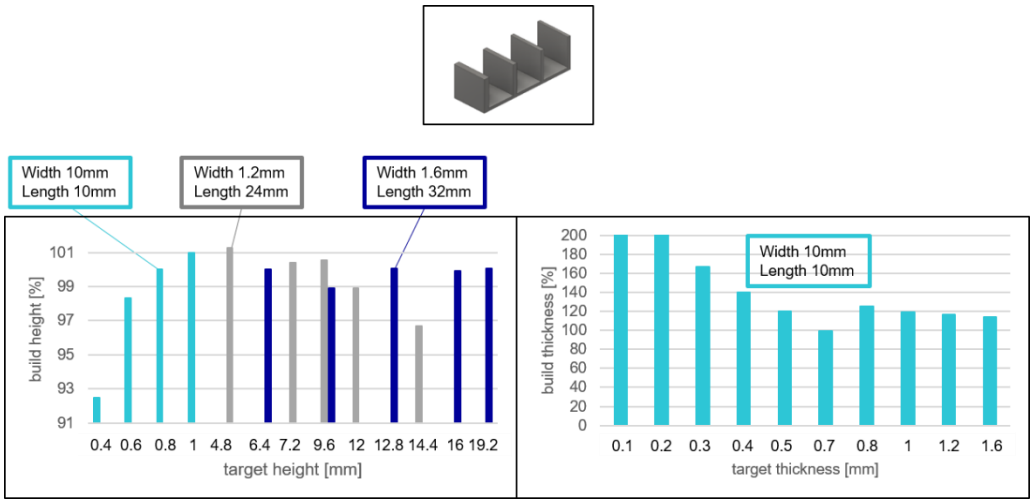

Figure 1: Height (left) and thickness (right) measurements for the unsupported walls.

Overhang, inclined walls and bridge features

The horizontal overhangs could only be produced up to an overhang length of 0.5 mm with a slight material droop in of up to 2 layers in height. Specimens with overhangs exceeding this value show disproportionate deformation of the overhangs. Figure 2 depicts an example of the defects of the straight overhangs, where the lowest filament layer sinks. Also, trying to use a different layer path in printing did not prevent the overhang from sinking.

Figure 2: Representation of the 0.5 mm (left), 1.0 mm (middle) and 2.0 mm (right) overhang and defects

Figure 3 illustrates a diagram of the average roughness values on the downskin surfaces, dependent of the overhang angle. The 0° overhang angle could not be produced. Due to the adhesion during printing with the build platform, overhangs of 15° are manufacturable. The average roughness Rz for the angle 15° is 376.6 µm, for 30° 423.6 µm. Therefore, it can be assumed that the average roughness value for 25° of 227.7 µm can be regarded as an outlier due to measurement inaccuracy. Starting at an overhang angle of more than 30° the average roughness of the downskin surface decreases noticeably. The surface for the overhang angle of 35° has a mean roughness Rz of 179,94 µm and for an overhang angle of 50° a mean roughness of 110.45 µm.

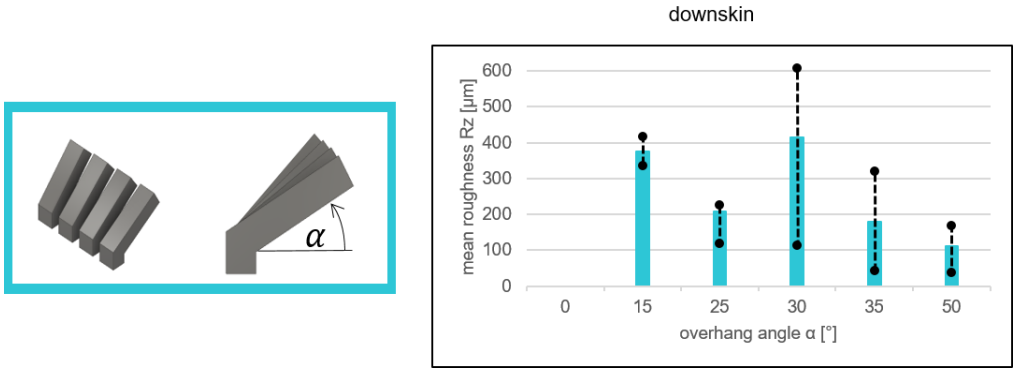

Figure 3: Mean Roughness measurements of the downskin surface for different overhang angle α.

The investigated bridge structures could all be manufactured and are depicted in figure 4. However, deformations are visible for bridge distances greater than 2 mm. With an unsupported bridge distance of 2 mm, it can be observed that individual filament strands sink distinctly. A microscope image of the 1.0 mm bridge distance illustrates the tendency of the lowest layer to bend already at this distance. (Fig. 4 bottom)

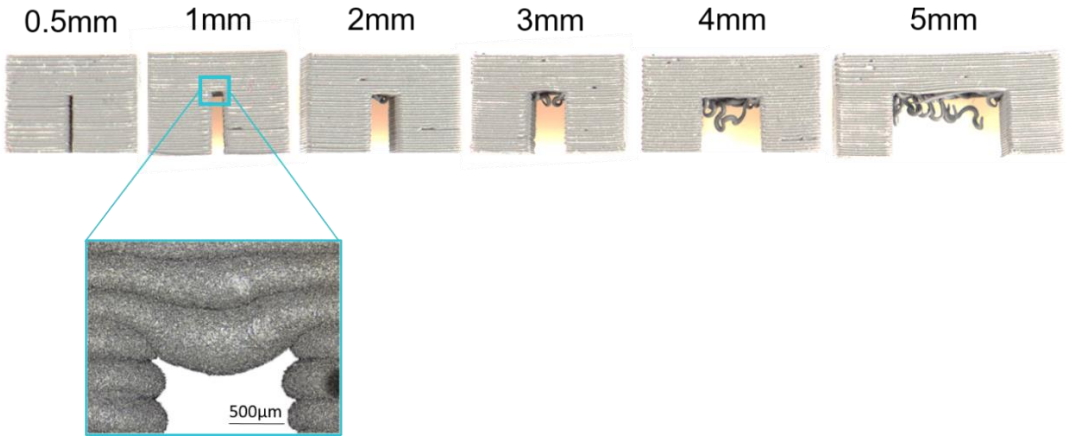

Figure 4: Investigated different bridge size geometries.

Cylindrical rods

The cylindrical rods could be manufactured for a thickness greater than 3 mm and are illustrated in Figure 5 (right). Narrower rods were not producible and tend to deform. In figure 5 (right), it can be seen that the percentage diameter of the created samples is constantly at 97% of the designed thickness. In Figure 5 on the left, different heights of the cylindrical rods have been manufactured. The small rods have a diameter manufactured with a height of 8 mm and the tall rods up to a height of 30 mm. All test geometries were successfully built. It can be observed that all specimens are higher than designed and approach the designed height incrementally. This deviation appears to decrease with increasing height, which could be a result of an over extrusion from the chosen slicer, the layer height and printing parameters.

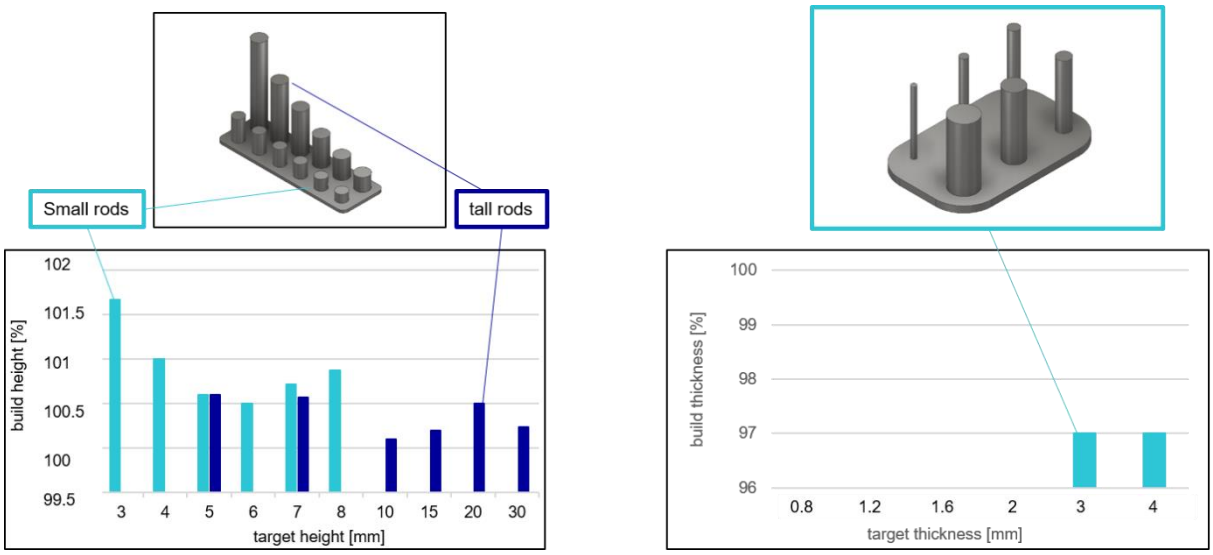

Figure 5: Measurements of the cylindrical rods.

Vertical gaps

The vertical gaps could be manufactured with a gap width of 0.3 mm to 0.5 mm. However, it can be observed that the widths of 0.5 mm are 43% smaller than the modeled widths. (fig. 6)

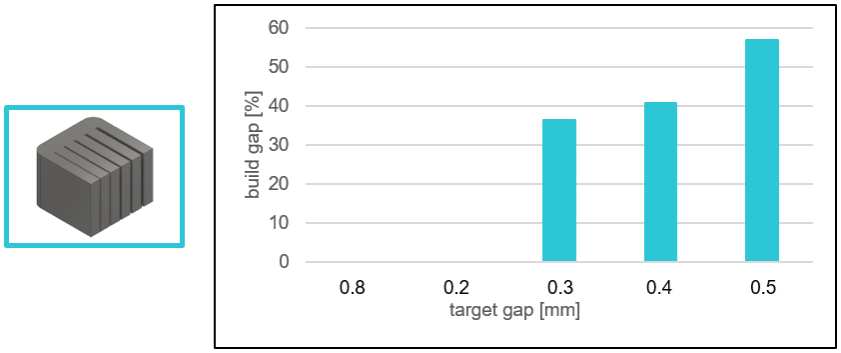

Figure 6: Measurements of the achieved width for vertical gaps.

One possible reason for this deviation is the extrusion of the filament through the nozzle. The material swells at the nozzle end and creates an overlap at the layer edge. It is hereby expected that the deviation can be reduced by using a smaller nozzle.

Boreholes

The diagram in Figure 7 displays the deviation of the diameter from the design in vertical and horizontal orientation. All boreholes could be manufactured in the vertical orientation except the borehole with a diameter of 0.8 mm. At a diameter size of 5 mm in vertical orientation no deviation from the design occurs. The diameters < 5 mm have all been manufactured smaller than designed. The reason for this is potentially the same as for the vertical gaps, where the material swells at the nozzle end and creates an overlap and the effective diameter is reduced.
The horizontal boreholes have been manufactured in the range of 1 mm – 4 mm. In this range the produced boreholes are significantly smaller than the designed. At a diameter of 4 mm, the layer of material in the overhang area sinks and a build-up is not possible. To overcome this failure support structures are needed.

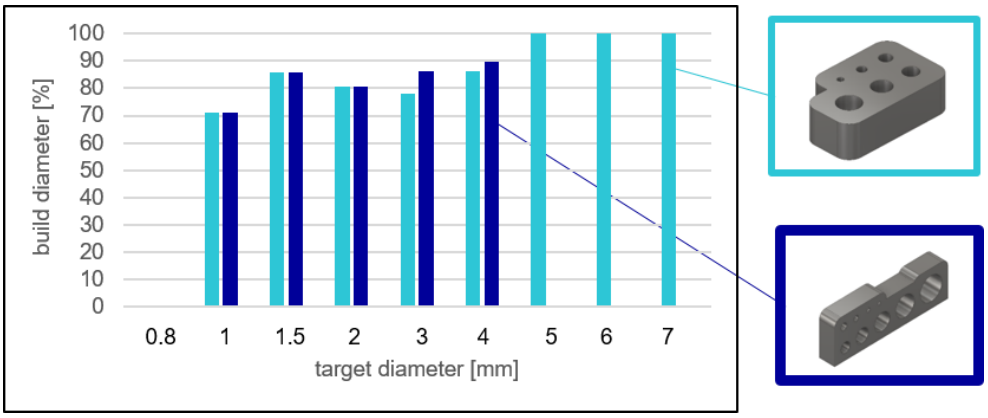

Figure 7: Borehole measurements of the diameter in different orientation.

Discussion

The results of the measurements allowed the development of design recommendations for AISI 316L (1.4404). For the design recommendations, the minimum deviations from the design have been defined as limits. This corresponds to a comparison to the design guidelines for piston-based metal printing [19] with an identical nozzle parameter and material. The results presented show some similarities e.g. vertical boreholes with a diameter of 1 mm can be manufactured and height limitations for unsupported walls in dependence of thickness. However, the results in [19] also show some disadvantages compared to filament-based extrusion. For example, cylindrical rods larger than 5 mm are to be constructed, whereas in the results shown above a build-up is already possible from 3 mm diameter. Furthermore, inclined walls can be produced from an angle of 35° and in piston-based only from an angle of 50°.
A further comparison with the design recommendations Markedforged [20] and Desktop Metal [21] indicates a transferability to the guidelines of this paper. Using the same 0.4 mm nozzle diameter, both guidelines give a recommendation for the cylindrical rods of 3 mm. The horizontal overhangs should be a maximum of 0.5 mm. The minimum wall thickness of the unsupported walls is 1.0 mm and the inclined walls should have a downskin angle of at least 40°. It can be assumed that the machine conditions have a smaller impact on the printable design than the material and process parameters.

Conclusion

Various design features have been manufactured in the MEX/M process using AISI 316L (1.4404). The experimental study of the features allows to identify the limitations for manufacture. Horizontal overhangs and bridges could be produced without a significant deviation with a length of 0.5 mm and 1.0 mm. Unsupported walls with a thickness of 1.6 mm are not limited by height. The inclined walls above 35° have a mean roughness of 310 µm. Cylindrical rods could be manufactured with 3 mm of the diameter, vertical boreholes 4 mm in diameter, while horizontal boreholes in the range of 1 mm to 4 mm were manufacturable. Vertical gaps larger than 0.5 mm show a higher design accuracy. The identified limits to the specimens allow a development of design guidelines for each feature.
With the help of the design recommendations, the knowledge about the process steps can be completed and a successful component design can be realized. Further research is planned for the extension of the design guideline for the debinding and sintering process steps for 316L (1.4404) and other materials. Also, demonstrators are being developed that will improve the mechanical properties related to design accuracy. The guideline is intended to ensure repeatability and save time in the production of a functional component.

Appendix Design Guideline Catalogue

Table 4: Design recommendation for the tested features with a nozzle size of 0.4 mm for AISI 316L (1.4404) after [13,15]. It is noticed that the guideline is specific to machine set-up, parameters and material especially with regard to the identified limits.

Geometry Feature		Recommendation	
Name	Illustration	Value	Comment
unsupported walls	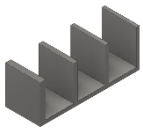	Wall thickness >1.6 mm Height thickness ratio < 12	• Produced thickness max. 15% higher for thickness of 1.6 mm (for 0.4 mm nozzle size) • Height to thickness ratio <12 for thicknesses <1.6 mm to prevent bending
Vertical gaps	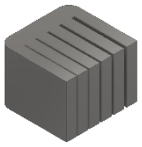	Width > 0.5 mm	• Negative width deviation of max. 43% of total width
Inclined walls	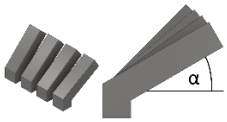	Overhang Angle ≥ 35°	• Manufacturable from 15° • **Downskin:** mean roughness max. ~610 µm for <35° and ~310 µm for 35° angle
Horizontal overhang		a ≤ 0.5 mm	• Overhang length > 0.5 mm must be supported to prevent material fall-in
Horizontal bridges	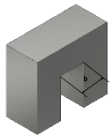	b ≤ 1.0 mm	• Bridge distance of 1.0 mm manufacturable • Greater bridge length should be supported to prevent the material from sinking
Cylindrical rods	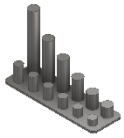	Diameter ≥ 3 mm	• Positive height deviation max. 1.5% of total height
Horizontal boreholes	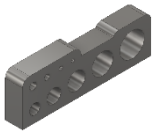	Diameter 1 mm – 4 mm	• No support structure necessary • For Diameter > 4 mm only with supportstructures manufacturable
Vertical boreholes	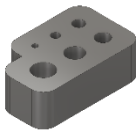	Diameter ≥ 4 mm	• For diameter in a range of 1 mm - 4 mm borehole size <25% smaller than total diameter • Diameter ≥ 5 mm produced borehole size meets the design

References

[1] Sargini, M.I.M.; Masood, S.H.; Palanisamy, S.; Jayamani, E.; Kapoor, A. Additive manufacturing of an automotive brake pedal by metal fused deposition modelling. Mater. Today Proc. **2021,** 45, 4601–4605.
[2] Khorasani, M.; Ghasemi, A.; Rolfe, B.; Gibson, I. Additive manufacturing a powerful tool for the aerospace industry. Rapid Prototyp. J. **2021,** 28, 87–100.
[3] BASF Ultrafuse, Available online https://www.ultrafusefff.com/product-category/metal/ultrafuse-316l/ (accessed on 26 April 2022)
[4] Virtual foundry, Available online https://filament2print.com/gb/45_the-virtual-foundry (accessed on 26 April 2022)
[5] Anycubic, Available online https://www.anycubic.com/products/316l-metal-filament-1-75mm (accessed on 26 April 2022)
[6] PT&A, Available online http://www.pt-a.de/ (accessed on 26 April 2022)
[7] Desktop Metal, Available online https://www.desktopmetal.com/products/studio (accessed on 26 April 2022)
[8] Triditive, Available online https://www.triditive.com (accessed on 26 April 2022)
[9] Markedforged, Available online https://markforged.com (accessed on 26 April 2022)
[10] Heaney, D.F. Handbook of Metal Injection Molding; Woodhead Publishing: Sawston, UK, 2018
[11] European Powder Metallurgy Association. Metal Injection Moulding: A Manufacturing Process for Precision Engineering Components; European Powder Metallurgy Association: Shrewsbury, UK, 2013
[12] C. Suwanpreecha, A. Manonukul, A review on material extrusion additive manufacturing of metal and how it compares with metal injection moulding, J 2022, 48-49
[13] J. Kranz, D. Herzog, and C. Emmelmann, Design guidelines for laser additive manufacturing of lightweight structures in TiAl6V4, J. Laser Appl. 27, S14001 (**2015**).
[14] L. Rebaioli and I. Fassi, A review on benchmark artifacts for evaluating the geometrical performance of additive manufacturing processes, Int. J. Adv. Manuf. Technol. 93, 2571–2598 (**2017**).
[15] D. Herzog, K. Asami, C. Scholl, C. Ohle, C. Emmelman, A. Sharma, N. Markovic, and A. Harris, Design guidelines for laser powder bed fusion in Inconel 718 (2021)
[16] Simplify3D, Available online https://www.simplify3d.com/support/print-quality-troubleshooting/stringing-or-oozing/ (accessed on 20 April 2022
[17] Simplify3D, Available online https://www.simplify3d.com/support/print-quality-troubleshooting/poor-bridging/ (accessed on 20 April 2022)
[18] All3DP, Available online https://all3dp.com/2/elephant-s-foot-3d-printing-problem-easy-fixes/ (accessed on 20 April 2022)
[19] C. Klemp, Systematic development of design rules for the production of green parts by means of piston-based feedstock extrusion, master thesis, 27 January 2021, Fraunhofer IAPT, TUHH iLAS
[20] Metal X design guideline, Available online https://assets-global.website-files.com/5b782089dfe0db977c49f302/60480ac3b3b559811a63ab4a_Markforged%20Metal%20Design%20Guide.pdf (accessed on 21 April 2022)
[21] BMD Design guide, Available online https://www.desktopmetal.com/uploads/Desktop-Metal-BMD-Design-Guide.pdf (accessed on 21 April 2022)